On: 12 November 2013, At: 01:12
Publisher: Taylor & Francis
Informa Ltd Registered in England and Wales Registered Number: 1072954 Registered office: Mortimer House, 37-41 Mortimer Street, London W1T 3JH, UK

Geomicrobiology Journal
Publication details, including instructions for authors and subscription information:
http://www.tandfonline.com/loi/ugmb20

An acidophilic bacterial-archaeal-fungal ecosystem linked to formation of ferruginous crusts and stalactites

Vasile Daniel Gherman [a] , Iulian Zoltan Boboescu [a] , Bernadett Pap [b] , Éva Kondorosi [b] , Gabriela Gherman [a] & Gergely Maróti [a b]

[a] "Politehnica" University of Timisoara, Hydrotechnical Engineering Department , Timisoara , Romania

[b] Hungarian Academy of Sciences, Biological Research Centre , Szeged , Hungary

Accepted author version posted online: 29 Oct 2013.Published online: 29 Oct 2013.

To cite this article: Geomicrobiology Journal (2013): An acidophilic bacterial-archaeal-fungal ecosystem linked to formation of ferruginous crusts and stalactites, Geomicrobiology Journal, DOI: 10.1080/01490451.2013.836580

To link to this article: http://dx.doi.org/10.1080/01490451.2013.836580

An acidophilic bacterial-archaeal-fungal ecosystem linked to formation of ferruginous crusts and stalactites

Short title: **Stalactite formation relies on the interaction of microbial community members**

Vasile Daniel Gherman[1], *Iulian Zoltan Boboescu*[1], *Bernadett Pap*[2], *Éva Kondorosi*[2], *Gabriela Gherman*[1] *and Gergely Maróti*[1,2#]

[1"]Politehnica" University of Timisoara, Hydrotechnical Engineering Department, Timisoara, Romania

[2]Hungarian Academy of Sciences, Biological Research Centre, Szeged, Hungary

E-mail: vasile.gherman@hidro.upt.ro (VDG), boboescu.iulian@yahoo.com (IZB), bernadett.pap@gmail.com (BP), eva.kondorosi@gmail.com (EK), gabi7gherman@yahoo.com (GG), maroti.gergely@brc.mta.hu (GM)

#Corresponding author:

Gergely Maróti

Temesvari krt. 62.

Szeged, 6726, Hungary

Phone: 0036308270455

Abstract

The presence of specialized microbial associations between populations of chemoautotrophic bacteria and archaea with ascomycetous fungi was observed inside stalactite-shaped mineral formations in a highly acidic cave environment. Metagenomic, chemical and electron microscopy analyses were used to investigate the relevance of these microbial ecosystems in the formation of stalactites. Ferric hydroxide produced by acidophilic bacteria and archaea was shown to be deposited onto fungal hyphae, resulting in complex mineralized stalactite-shaped structures. Thus, both archaeal-bacterial and fungal members of the ecosystem were shown to play an active role in the formation of stalactites.

Keywords: ferruginous stalactites, metagenomics, bacterial-fungal interaction (BFI), acidophilic archaea,

1. Introduction

Among the Earth's extreme environments, hyper-mineralized caves of acidic pyrite rock drainage represent important models in the field of geomicrobiology (Johnson, 1998). Extremophile organisms that inhabit such environments require drastic adaptation strategies that tend to involve morphological and genetic alterations (Johnson et al. 2001). Rainwater slowly infiltrates through microcracks in the rocks, reaching the cave ceiling as a highly concentrated acidic solution (pH 1-2) soured by mainly H_2SO_4 as a result of various oxidation reactions of chemolithotrophic sulfur metabolism.. The metabolic processes and various ecologic interactions among microbial populations inhabiting these acidic pyrite environments are extremely complex. Primary producers are typically comprised of iron- and sulfur-oxidizing chemolithotrophic bacteria and archaea (*Acidithiobacillus* spp., *Leptospirillum* spp., *Ferroplasma* spp., *Thermoplasma* spp., etc.) (Brett and Jillian, 2003). Fixed carbon generated by these primary producers is used by heterotrophic acidophilic microorganisms, such as bacteria from *Acidiphilium* sp. as well as various *Hyphomycetes* and melanized *Ascomycetes* fungi, to stimulate the growth of chemolithotrophs by removing the soluble organic compounds (Rawlings, 1999; Ehrlich, 2002). Thus, mixed populations of acidophilic microorganisms inhabit these extreme environments more efficiently than pure cultures. The endproducts generated by members of these complex microbial populations are used as electron donors or acceptors by other inhabitants. For instance, iron-oxidizing bacteria oxidize the reduced iron, and the resulting compounds are used by the iron-reducing species as terminal electron acceptors (Ehrlich, 2002). Microbial oxidation of reduced metallic compounds is thermodynamically more favorable than chemical oxidation.. The oxidized metal compounds are often deposited (actively or passively) in

various negatively charged extracellular structures synthesized in large quantities by extremophilic microorganisms (Ferris et al. 1987; Ferris et al. 1988). As a consequence, mineral deposits of biogenic origins are formed.

The role of microorganisms in secondary mineral formation has been characterized extensively (Ferris et al. 1989; Beveridge, 1989; Urrutia and Beveridge, 1994; Schultze-Lam et al. 1996; Fortin et al. 1997). It is widely recognized that several important mineral transformations, like smectite transformation to illite clay and the generation of iron, uranium and gold deposits, which were originally considered to be inorganic in nature, are mediated by microbial communities (Kim et al. 2004; Newman and Banfield, 2002). Recent studies have shown that certain bacteria, archaea as well as fungi, are able to precipitate and deposit crystalline and amorphous material in and around their cell walls and surface layers. These minerals of biogenic origin include carbonates, oxalates, hydroxides, phosphates and sulfides (Burford et al. 2003a; Burford et al. 2003b; Burford et al. 2006; Benzerara et al. 2011). Fungi and bacteria can effectively oxidize and precipitate Mn(II) and Fe(II) (de Rome and Gadd, 1987; Morley and Gadd, 1995; Spilde et al. 2005; Barton and Northup, 2007). The oxidized metal layer, called desert varnish, is also considered to be of microbial origin (Wang et al. 2011; Parchert et al. 2012).

Acid mine drainage (AMD) is formed when metal sulfide minerals, particularly pyrite (FeS_2), are exposed to oxygen and water. Generally, the rate of inorganic oxidation of ferrous iron (Fe^{2+}) in AMD is low, especially at low pH (i.e. below a pH of 3). However, certain acidophilic organisms can generate energy by converting ferrous iron to ferric iron (Fe^{3+}) (Johnson et al. 2001; Brett and Jillian, 2003). Thus, the oxidation of pyrite and acidification of AMD is greatly

increased in the presence of acidophilic organisms, such as the iron-oxidizing species *Acidithiobacillus ferrivorans*, *Acidithiobacillus ferrooxidans* and *Ferroplasma acidophilum* (Johnson, 1998; Johnson et al. 2001; Brett and Jillian, 2003). *A. ferrooxidans*, a well-studied organism, catalyzes the oxidation of pyrite and acidification of AMD. In the recent years, models have been proposed for its energetic characteristics and its role in pyrite dissolution (Johnson, 1998; Johnson et al. 2001; Brett and Jillian, 2003; Ehrlich, 2002). Until recently, *A. ferrooxidans* has been considered the major microorganism responsible for the extreme acidic conditions of AMD systems. However, recent molecular ecology studies revealed the significance of additional iron-oxidizing microorganisms, such as *Thiobacillus* spp., *Leptospirillum* spp., *Ferrovum* spp. and *Ferroplasma* spp. In certain environments, these strains were shown to contribute more to acid production than *A. ferrooxidans* (Schrenk et al. 1998; Edwards et al. 2000).

In addition to prokaryotes, fungi were also shown to be involved in the dissolution of inorganic materials, which is mostly explained by their morphological and physiological flexibility and also by their ability to create various symbiotic relationships (Sayer et al. 1999; Ehrlich, 2006; Gadd et al. 2007; Gadd, 2007; Gadd, 2008; Gadd, 2010). Even in the harshest environments, fungi are fundamental components of all rock types. Fungi often coexist and interact with bacteria. Certain associations lead to formation of biofilms on various inorganic materials. Specifically, fungi-bacteria interactions may lead to the formation of crusts and complex mineral structures on rocks and mineral surfaces (Gorbushina et al. 2003; Gorbushina, 2007). Fungal attack and colonization occur through hyphal penetration (Bowen et al. 2007; Gadd and Raven, 2010). Additionally, fungi can function as dissolution agents through metabolite

excretion, including H^+, carboxylic acids, CO_2, siderophores, amino acids and phenolic compounds (Gadd, 2007; Gadd, 1999).

It is critical to determine the contribution of microbial communities in the leaching of different minerals from source rock, clarifying their possible role in the precipitation of such minerals. Thus, the current study examined the role of a special microbial consortium of various bacteria, archaea and fungi species in the mobilization of sulfur and iron, as well as the precipitation of their oxidized forms into complex stalactite-shaped mineral deposits. Determining the extent of microbial involvement in the formation of the mineral deposits in such cavities may provide an indication of the possible biogenic origins of such stalactite-shaped structures. Based on experimental data, a direct relationship between the development of mineral deposits (crusts and stalactites) and the metabolism of the microbial communities is proposed.

2. Materials and Methods

2.1. Sample sites and sampling procedures

Samples were obtained from an old mine (Kiesberg Mine) located in the South-West of Romania in the Banat Mountains that was abandoned at the end of the 19th century (Fig. 1). The mine is located in the auriferous sulfides of Policarpus ore within metamorphic rocks. Policarpus ore mineralization is primarily made of pyrite and pyrrhotite as well as of chalcopyrite, cobaltine and marcasite.

Biological and geological sampling was done in order to isolate and identify the microbial communities living in the investigated area, as well as geologically characterize the environment. Sampling points were located at a distance of approximately 40m from the mine

entrance. The temperature in Kiesberg Mine is 15°C steadily throughout the year. The pH of the sampled microenvironment is ranging between 1 and 2. Droplets of percolation solution at the tips of stalactites were aseptically sampled using sterile tools, gloves and tubes in order to assess the microbial biodiversity of the microenvironment. Samples of percolation solution, together with different types of mineral deposits, were also acquired for geochemical composition analyses.

2.2. Isolation of microorganisms

In situ inoculations onto both solid and liquid media were performed at the sampling site. The following media were used: solid and liquid yeast and malt extract with glucose media (YMG), solid and liquid potato and glucose media (PG), solid and liquid Sabouraud media, solid and liquid Man, Rogosa and Sharpes media (MRS), solid and liquid malt and potato media MP, as well as solid and liquid Czapek-Dox media. Plates were solidified with 1.5% agar and adjusted to either pH 7.2 or 5. Percolation solution (0.1 ml) from the tips of stalactites was spread on each plate using tenfold serial dilution(logarithmic dilution) of 4 steps with the first step being the concentrated solution.. Plates were incubated at 30°C overnight both aerobically and anaerobically.

2.3. Extraction of environmental DNA

Total microbial DNA of the sampled environment was extracted as previously described by Sharma et al. (2010) with minor modifications to the methodology. For selective isolation of high quality total prokaryotic DNA from samples (0.5 g), 1.3 ml extraction buffer (100 mM Tris

Cl, pH 8.0, 100 mM EDTA, pH 8.0, 1.5 M NaCl, 100 mM sodium phosphate, pH 8.0, 1% CTAB) supplemented with 7 µl proteinase K (20.2 mg/ml) was used. After incubation at 37°C for 45 min, 160 µl 20% SDS was added and mixed by inversion. The sample mixture was then incubated at 60ºC for 1 h with intermittent shaking every 15 min. Samples were centrifuged at 13,000 rpm for 5 min, and the supernatant was transferred into clean Eppendorf tubes. The remaining soil pellets were treated three times with 400 µl extraction buffer and 60 µl SDS (20%), then incubated at 60ºC for 15 min with intermittent shaking every 5 min. The supernatants collected from all extraction steps were mixed with an equal amount of chloroform and isoamyl alcohol (25:24:1). The aqueous layer was separated and precipitated with 0.7 volume of isopropanol. After centrifugation at 13,000 rpm for 15 min, the brown pellet was washed with 70% ethanol, dried at room temperature and dissolved in TE (10 mM Tris Cl, 1 mM EDTA, pH 8.0).

Fungi DNA was extracted from a mix offungi colonies grown on solid media. The SOLEX Special® Genomic DNA Isolation Kit for plants and fungi (provided by Institute of Isotopes Co. Ltd.) was used for the extraction with the following modifications: after rinsing the pellets, samples were dried under vacuum for 10 min at 30°C. Subsequently, 75 µl water was added and the DNA was rehydrated at 65°C for 10 min. Further, the samples were centrifuged for 3 min, and the supernatant was carefully transferred into a new vial without disturbing the pellet.

2.4. Characterization of the community composition based on 16S/18S rRNA

Bacterial, archaeal and fungi specific 16S/18S rRNA PCR (f27 5'-AGAGTTTGATCCTGGCTCAG-3' and r1492 5'-ACGGCTACCTTGTTACGACTT-3', 63F 5′-CAGGCCTAACACATGCAAGTC-3', 1542R 5′-AAGGAGGTGATCCAGCCGCA-3' for bacteria; UA571F 5'-GCYTAAAGSRICCGTAGC-3' and UA1204R 5'-TTMGGGGCATRCIKACCT-3' for archaea; NS1 5'-GTAGTCATATGCTTGTCTC-3' and NS2 5'-GGCTGCTGGCACCAGACTTGC-3' for fungi) reactions were performed on both the colonies grown on plates and on isolated total environmental DNA to estimate the microbial composition of the collected samples. Capillary Sanger sequencing on isolated PCR products was used to determine the exact sequence of the amplified 16S/18S rRNA fragments. BLAST (http://blast.ncbi.nlm.nih.gov/) homology searches were used to identify sequences.

2.5. Sequence-based metagenomics

Total environmental DNA extracted from the collected samples (prokaryotic and fungi DNA separately) were prepared for high-throughput next-generation sequencing using a SOLiD V4 (Life Technologies) Next Generation Sequencer (NGS). The short raw DNA sequences generated by parallel sequencing (2,963,364 short reads with a mean read length of 46.1 nucleotides, totaling 136,611,080 bases) were assembled into contigs using CLC Bio Genomics WorkBench software (www.clcbio.com). The 4,442 contigs (mean sequence length of 312 +/- 129 nt) were used to create environmental gene tags (EGTs) and clusters of orthologous groups of proteins (COGs). Bioinformatic analyses (taxonomic profiling, assessment of metabolic potential) were conducted using the public MG-RAST software package, which is a modified version of RAST (Rapid Annotations based on Subsystem Technology)

(http://blog.metagenomics.anl.gov/tools-and-data-used-in-mg-rast). Data were normalized, processed and evaluated by aligning contigs using several public SSU, LSU, whole genome and metagenome databases.

2.6. Determination of mineral composition

Chemical analyses were performed using atomic absorption spectrometry (Varian Spectraa 880, ecro System, Romania). The following elements were measured in each sample (in $mg \cdot L^{-1}$): Fe, Na, K, Cr, Cd, Ni, Pb, Zn, Mn and Cu.

2.7. TEM and SEM analysis of mineral structures

Scanning electron microscopy (SEM) and transmission electron microscopy (TEM) were performed on biological and geological samples collected from the selected area in order to visually confirm possible associations between the microorganisms living in the stalactite structures, as well as to characterize the internal morphology of mineral structures. Samples for electron microscopy were prepared by standard methods previously described by McDowell and Trump (1976).

A LEO Gemini (Zeiss DSM 982; Carl Zeiss SMT, AG Oberkochen, Germany) scanning electron microscope, as well as a JEOL 1011 and JEOL 1230 (JEM 1011, JEOL Europe S.A., CCD Gatan ES 1000 W Erlangshen camera; big angle; JEM 1230, JEOL Europe S. A., CCD Gatan Bioscan camera; big angle) transmission electron microscopes were used in the current study. SEM observations were coupled with energy dispersive spectrometry (EDS X-ray detector Pioneer (Noran), Elexience; IDfix Software, SAMX Microanalysis Application Software,

Levens, France). Samples were coated with Pt (~0.9 nm thickness) and examined under an accelerating voltage of 15 kV with a working distance of 16 mm. TEM samples were prepared using the Ultracut E Reichert ultramicrotome, and observations were made at an accelerating voltage of 80 kV. The three-dimensional architecture of the acidophilic microbial communities, as well as the interactions between the microbes and the mineral structures, were investigated by SEM. Cross-sections of biological structures where different minerals were deposited, as well as the interactions between these structures and the microorganisms, were subjected to TEM analysis.

3. Results

Percolation solution is rainwater that has dissolved several minerals to create a highly acidic environment, facilitating formation of crusts and speleothems (stalactites) (Fig. 2). Specifically, crusts form on the mine ceiling, starting in the highly concentrated acid percolation solution (Fig. 2A and B). The color of the percolation solution at the tip of the stalactites can vary from orange to ruby red. White filaments, representing fungal hyphae, were detected in these drops (Fig. 1D). Chemical, microbiological and metagenomic analyses were performed on the percolation solution to investigate the ecosystem of this special environment. Electron microscopy studies were carried out on the stalactites in order to provide support for the role of the microbial communities in the development of these structures.

3.1. Chemical composition of the percolation solution

The pH of the percolation solution ranged from 1–2, indicating extremely acidic conditions. Atomic absorption spectroscopy was used to measure the concentration of inorganic compounds in the solution. Results showed particularly high levels of Fe, Cu, Mn and Zn (Table 1.) Thus, this solution represents an extreme environment suitable for microorganisms with special metabolic capabilities, such as ferrous iron oxidation, sulfur oxidation as well as manganese oxidation.

3.2. Metagenomic analysis of microbial communities

The acidic percolation solution showed an increased superficial tension due to the high concentration of ferrous iron and other elements, and formed a continuous 0.5 mm thick layer on the surface of the cavity ceiling, as well as droplets on the tips of small stalactites. These highly acidic droplets were analyzed by high-throughput sequencing-based metagenomics. Taxonomic profiling performed on sequences aligned to ribosomal subunits showed the presence of a complex microbial community composed of diverse bacterial groups, typical acidophilic archaeas and ascomycetous fungi (Fig. 3 and Table 2). Members of the chemolithotrophic *Leptospirillum* genus (Nitrospirae phylum) were shown to be the most abundant bacterial components (24% of the total bacterial-archaeal community) followed by those of *Acidithiobacillus* (from Gammaproteobacteria class) (5%). The most abundant bacterial species of the identified community were *Leptospirillum rubarum,* Leptospirillum sp. Group II, *Leptospirillum ferrodiazotrophum*, *Acidithiobacillus ferrooxidans* and *Acidithiobacillus caldus*. Interestingly, high bacterial diversity was observed in the sampled environment, various kinds of further Proteobacteria (mainly from *Geobacter*, *Nitrospira, Burkholderia* and *Pseudomonas*

genera, each counting for 2-3% of the total bacterial-archaeal ecosystem) as well as a few members of the Firmicutes phyla (*Clostridium* and *Bacillus* genera, 1-2% each) were detected in significant amount (Fig.3 and Table 2). The archaeal acidophils were represented by high numbers of *Ferroplasma* spp., *Thermoplasma* spp., *Picrophilus* spp. and *Sulfolobus* spp., each counting for about 2-3% of the total bacterial-archaeal community (Table 2). The fungi partners of the association were exclusively represented by the *Penicillium* genus, *Penicillium oxalicum*, *Penicillium purpurogenum*, *Penicillium camemberti* and *Penicillium corylophilum* were detected (Fig. 3). This co-localization of ascomycetous fungi with metal- and sulfur-oxidizing bacteria and archaea was hypothesized to be a functional association at the investigated sulfur and metal rich environment.

3.3. Microscopy studies on the stalactite development

Microscopy analyses were performed to support the hypothesis based on the metagenomics data. Macroscopic analysis of the stalactite-type formations provided an initial indication that crusts and stalactites on the cave ceiling were formed by superimposed ferric hydroxide layers (Fig. 4A and B).

Each superimposed ferric hydroxide layer was composed of two alternating surfaces. The first one corresponds to a massive, completely mineralized dense layer, while the second surface was composed of scattered fiber-like structures with mineralized fungal hyphae.

Crusts enhance the formation of microbial communities on the cave ceiling by offering an irregular binding surface and a continuous thick layer of acidic percolation solution. Here, the developing microbial biofilm forms droplets at protrusions from the ceiling, initiating the

formation of stalactites. The biofilm is stable since it is supplied extremely slowly by the percolation water and also because of the high concentration of dissolved substances (Fig. 5B). The thickness of the ferric hydroxide layer ranges from a few tens to a few hundreds of microns. As shown by its final laminated structure (Fig. 5A), the layer is slowly formed over time and shows a discontinuous pattern. While this layer is formed at the biofilm exterior, the ferric hydroxide is being precipitated on the fungal hyphae inside the biofilm. These hyphae give a curly aspect to the crusts and are visible inside the stalactites (Fig. 5C and D).

Mineralization of fungal hyphae occurs at their exterior, starting from the wall then displaying a radial pattern that extends distally. Each fiber progressively thins out until eventually reaching a hair-like thickness, which results in the fluffy look of the hyphae (Fig. 6A). Once completely mineralized, the hyphae degrade, leaving a single lumen (Fig. 6A). TEM examination of the fungal hyphae sampled from the drops formed at the tips of stalactites allowed us to detect the first stages of ferric hydroxide deposition upon the cellular wall. The minerals were displayed in hair-like formations encrusting the periphery of the hyphae (Fig. 6B–D).

Both the base and body of stalactites were filled with percolation solution. This solution is constantly supplied with Fe^{2+}, allowing the propagation of chemolithotrophic bacteria. The pin-shaped mineralization of fungal hyphae serves as a physical support for the percolation solution (Fig. 5C and D). Drops from the tip of the stalactites were filled with numerous chemolithotrophic bacteria, mainly from *Leptospirillum* and *Acidithiobacillus* genera, as well as pervasive fungal hyphae (Fig. 3). Upwards in the mineralized stalactite, fossil bacteria are scattered along the mineralized hyphae (Fig. 5D).

The hyphae transformation involved during ferruginous stalactite formation can be detected in the micro-zone (the base of a droplet situated on the tip of a stalactite), where the mineralization process is active and living hyphae coexist with mineralized hyphae (Fig. 7A). The living fungal hyphae displayed numerous fine filaments of various shapes that protruded from the wall with a length up to several microns. Certain filaments were particularly long (2–4 μm) and twisted around the hyphae. Direct physical contact between the filaments of the fungi and bacteria was often observed, supporting the possibility of a trophic association between these organisms. (Fig. 7B–D).

4. Discussion

Caves are considered extremely starved environments due to the geologic isolation and the absence of sunlight. The levels of available organic carbon are extremely low, thus heterotrophic microbial growth is very limited. Microbes residing under such starved conditions developed a wide range of unconventional energy conserving reactions to utilize the available - mostly inorganic - materials through reducing the minerals within the rock of the cave (Barton et al. 2004, Chelius and Moore, 2004; Northup et al. 2003). Extreme acidophiles are widely distributed throughout the three Domains of life, their representatives from *Eukarya*, *Archaea* and *Bacteria* display a wide range of metabolic activities (use of solar or chemical energy, inorganic or organic carbon, growth in the presence or absence of oxygen) depending on the environment (Johnson, 2012). Here we have assessed the microbial diversity of a sulfuric cave environment and proposed the concerted metabolic activities of bacterial, archaeal and fungal components in the formation of stalactites.

The functionality of the investigated cave ecosystem consisting mainly of chemolithotrophic *Leptospirillum* and *Acidithiobacillus* bacteria together with *Ferroplasma* and *Thermoplasma* acidophilic archaea and *Penicillium* fungi is based on the oxidation of various metal sulfides in the metamorphic rock layer on the cavity ceiling. Further bacterial groups were identified in the environment, the presence of various *Proteobacteria* (basically soil bacteria e.g. members of *Geobacter*, *Shewanella*, *Pseudomonas* genera) as well as the Gram-positive *Clostridium* and *Bacillus* strains, might also be connected to the oxidative processes in this specific cave or might simply be explained by the possible availability of various organic carbon sources.

Microcracks on the ceiling are permanently filled with acidic percolation solution, providing an ideal environment for chemolithotrophic bacteria. Some of these bacteria are attached to pyrite, chalcopyrite or marcasite minerals in the rock mass, while others dwell in the solution. *Penicillium* species were found residing alongside these chemolithotrophic bacteria on the cavity ceiling, as well as on stalactites.

Metal biosolubilization is performed enzymatically by microorganisms in direct contact with the pyrite crystal (Ehrlich, 2006). Microbial oxidation of pyrite by bacteria attached to the crystal is described by the following equation (1):

$$FeS_2 + 3.5O_2 + H_2O \xrightarrow{\text{bacteria}} Fe^{2+} + 2H^+ + 2SO_4^{2-} \quad (1)$$

The Fe^{2+} generated is then oxidized by bacteria living in the percolation solution, as shown in equation (2). The solution is supposed to reach the cavity ceiling, leading to formation

of a microbial consortium dominated by chemolithotrophic bacteria and archaea (supposedly mainly by *Leptospirillum* and *Ferroplasma*) and *Penicillium* fungi (most probably *Penicillium oxalicum*).

$$2Fe^{2+} + 0.5O_2 + 2H^+ \xrightarrow{\text{bacteria}} 2Fe^{3+} + H_2O \quad (2)$$

A large number of bacterial cells were observed using SEM analysis. Such bacteria were either closely associated with the fungal hyphae towards the tip of the ferruginous stalactites or located in the percolation solution collecting at the tip of the stalactites (Fig. 7C and D). Thus, in order to maintain the metabolism of the microbial consortium, which facilitates formation of crusts and stalactites on the ceiling, large quantities of Fe^{2+} must be supplied from the cavity rock mass. Chemical oxidation of the residual pyrite further increases the amount of Fe^{2+} available for the chemoautotrophic bacteria, as shown in equation (3):

$$FeS_2 + 14Fe^{3+} + 8H_2O \rightarrow 15Fe^{2+} + 2SO_4^{2-} + 16H^+ \quad (3)$$

This process represents the indirect biooxidation of pyrite. Fe^{2+} generated by direct and indirect biosolubilization of pyrite is oxidized to Fe^{3+} at the tip of stalactites by the bacterial consortium, as shown in equation (2).

Fe^{3+} forms ferric hydroxide which precipitates and mineralizes the fungi hyphae as shown in equation (4):

$Fe^{3+} + 3H_2O \rightarrow Fe(OH)_3 + 3H^+$ (4)

The investigated mine is located in a magma intrusion covered by a several meters thick calcareous layer. An especially rich soil resides on the top of this layer completely covered with luxuriant vegetation. This specific geomorphology likely results in a percolation water enriched with organic substrates. This water reach the stalactites delivering all required nutrients to the fungal component of the consortium. In addition to this external source of organic nutrients, a mutual trophic association between bacteria and fungi is suggested by the fact that there is an intimate contact between the fungal hyphae extensions and the bacterial-archaeal community. These extensions may serve as channels between the fungi and the chemolithotrophic bacteria and archaea, where various metabolic products may be exchanged. The percolating water could also play a crucial role in the initial fungal colonization of the stalactite forming positions. The extremely low pH values detected in the stalactite droplets seems to have limited inhibitory activity on the growth of the fungal species. The observation that living fungal hyphae colonized the tip of the stalactites during all stages of stalactite development, as well as the fact that fossilized fungal hyphae are forming the body of the stalactites, might support this theory.

Chemolithotrophic bacteria are also able to use sulfur and sulfides from the cavity ceiling as energy sources. Moreover, metabolism of elementary sulfur (S^0) provides greater energy than Fe^{2+} (Ehrlich, 2006). Elementary sulfur is converted to sulfuric acid by different *Leptospirillum* and *Acidithiobacillus* bacteria together with *Ferroplasma* and *Thermoplasma* archaea, thereby increasing the acidity of the percolation solution according to equation (5):

$$S^0 + 1.5O_2 + H_2O \xrightarrow{bacteria} H_2SO_4 \quad (5)$$

The laminated structure of the crusts and stalactites implies a discontinuous growth. This can be explained by an autocyclic process in which the described bacterial-fungal association is gradually mineralized, thus stalactites form through an iterative development of the biofilm on the growing crust surface.

5. Conclusion

The acidic percolation solution collected in the described cave environment contained an acidophilic community of microorganisms, illustrating a complex association between chemolithotrophic bacteria, acidophilic archaea and ascomycetous fungi species. The ferric hydroxide formed by the chemolithotrophic bacteria was most likely deposited on the exterior of fungal hyphae through the oxidation of pyrite, thus forming complex mineral structures, such as ferruginous crusts and stalactites. These mineral structures are an example of mineral precipitation based on the association of various microorganisms. The proposed highly concerted and finely tuned cooperation of various microorganisms points to the flexibility and adaptation ability of microbes to highly specific conditions. Additional studies using high-throughput transcriptome-based analyses may reveal the nature and extent of this symbiotic interaction.

6. Acknowledgements

We thank JG Breheret, B Arbeille, P Roingeard, P-Y Sizaret, P-I Raynal, C Lebos, M Lemesle, S Trassard, and F Arcanger for their contribution and help with preparation of samples for electron microscopy. This research was partially supported by the French Government, the Bucharest Biology Institute of the Romanian Academy, GéEAC Laboratory of François-Rabelais University (Tours, France), as well as the following international (EU) and domestic (Romanian and Hungarian) funding sources: "SYMBIOTICS" ERC AdG EU grant and the strategic grant "POSDRU" 107/1.5/S/77265, inside POSDRU Romania 2007-2013 co-financed by the European Social Fund – Investing in People.

7. References

Barton HA, Northup DE. 2007. Geomicrobiology in cave environments: past, current and future perspectives. J Cave Karst Stud. 69:163-178.

Barton HA, Taylor MR, Pace NR. 2004. Molecular phyloge-netic analysis of a bacterial community in an oligotrophic cave environment. Geomicrobiol J. 21:11–20.

Benzerara K, Miot J, Morin G, Ona-Nguema G, Skouri-Panet F, Ferard C. 2011. Significance, mechanisms and environmental implications of microbial biomineralization. C R Geosci. 343:160-167.

Beveridge TJ. 1989. Interactions of metal ions with components of bacterial cell walls and their biomineralization. In: Poole RK, Gadd GM (ed), Metal-Microbe Interactions, IRL Press, Oxford, UK, p. 65-83.

Bowen AD, Davidson FA, Keatch R, Gadd GM. 2007. Effect of nutrient availability on hyphal maturation and topographical sensing in *Aspergillus niger*. Mycoscience. 48:145-151.

Brett JB, Jillian FB. 2003. Microbial communities in acid mine drainage. *FEMS* Microbiol Ecol. 44:139-152.

Burford EP, Fomina M, Gadd GM. 2003a. Fungal involvement in bioweathering and biotransformation of rocks and minerals. Mineral Mag. 67:1127-1155.

Burford EP, Hillier S, Gadd GM. 2006. Biomineralization of fungal hyphae with calcite ($CaCO_3$) and calcium oxalate mono- and dihydrate in carboniferous limestone microcosms. Geomicrobiol J. 23:599-611.

Burford EP, Kierans M, Gadd GM. 2003b. Geomycology: fungal growth in mineral substrata. Mycologist. 17:98-107.

Chelius MK, Moore JC. 2004. Molecular Phylogenetic Analysis of Archaea and Bacteria in Wind Cave, South Dakota. Geomicrobiol J. 21:123–134.

de Rome L, Gadd GM. 1987. Copper adsorption by *Rhizopus arrhizus*, *Cladosporium resinae* and *Penicillium italicum*. Appl Microbiol Biotechnol. 26:84–90.

Edwards KJ, Bond PL, Gihring TM, Banfield JF. 2000. An archaeal iron-oxidizing extreme acidophile important in acid mine drainage. Science. 287:1796-1799.

Ehrlich HL. 2002. Geomicrobiology. 4th edition, New York, Marcel Dekker.

Ehrlich HL. 2006. Geomicrobiology: relative roles of bacteria and fungi as geomicrobial agents. *In* Gadd GM, (ed), Fungi in Biogeochemical Cycles: Cambridge University Press, Cambridge, UK, p. 1-27.

Ferris FG, Fyfe WS, Beveridge TJ. 1987. Bacteria as nucleation sites for authigenic minerals in a metal-contaminated lake sediment. Chem Geol. 63:225-232.

Ferris FG, Fyfe WS, Beveridge TJ. 1988. Metallic ion binding by *Bacillus subtilis*: implications for the fossilization of microorganisms. Geology. 16:149-152.

Ferris FG, Schultze S, Witten TC, Fyfe WS, Beveridge TJ. 1989. Metal interactions with microbial biofilms in acidic and neutral pH environments. Appl Environ Microb. 55:1249-1257.

Fortin D, Ferris FG, Beveridge TJ. 1997. Surface-mediated mineral development by bacteria. Rev Mineral. 35:161-180.

Gadd GM. 1999. Fungal production of citric and oxalic acid: importance in metal speciation, physiology and biogeochemical processes. Adv Microb Physiol. 41:47-92.

Gadd GM. 2007. Geomycology: biogeochemical transformations of rocks, minerals, metals and radionuclides by fungi, bioweathering and bioremediation. Mycol Res. 1113-49.

Gadd GM. 2008. Bacterial and fungal geomicrobiology: a problem with communities? Geobiology. 6:278-284.

Gadd GM. 2010. Metals, minerals and microbes: geomicrobiology and bioremediation. Microbiol. 156:609-643.

Gadd GM, Dyer P, Watkinson S. 2007. Fungi in the Environment. Cambridge University Press, Cambridge.

Gadd GM, Raven JA. 2010. Geomicrobiology of eukaryotic microorganisms. Geomicrobiol J. 27:491-519.

Gorbushina AA. 2007. Life on the rocks. Environ Microbiol. 9:1613-1631.

Gorbushina AA, Whitehead K, Dornieden T, Niesse A, Schulte A, Hedges JI. 2003. Black fungal colonies as units of survival: hyphal mycosporines synthesized by rock-dwelling microcolonial fungi. Can J Bot. 81:131-138.

Johnson DB. 1998. Biodiversity and ecology of acidophilic microorganisms. FEMS Microbiol Ecol. 27:307-317.

Johnson DB, Rolfe S, Hallberg KB, Iversen E. 2001. Isolation and phylogenetic characterization of acidophilic microorganisms indigenous to acidic drainage waters at an abandoned Norwegian copper mine. Environ Microbiol. 3:630-637.

Johnson DB. 2012. Geomicrobiology of extremely acidic subsurface environments. FEMS Microbiol Ecol. 81:2-12.

Kim J, Dong H, Seabaugh J, Newell SW, Eberl DD. 2004. Role of microbes in the smectite-to-illite reaction. Science. 303:830–832.

McDowell EM, Trump BF. 1976. Histologic fixatives suitable for diagnostic light and electron microscopy. Int J Syst Evol Micr. 100:405-414.

Morley GF, Gadd GM. 1995. Sorption of toxic metals by fungi and clay minerals. Mycol Res. 99:1429-1438.

Newman DK, Banfield JF. 2002. Geomicrobiology: How molecular-scale interactions underpin geochemical systems. Science. 296:1071–1077.

Northup DE, Barns SM, Yu LE, Spilde MN, Schelble RT, Dano KE, Crossey LJ, Connolly CA, Boston PJ, Dahm CN. 2003. Diverse microbial communities inhabiting ferromanga-nese deposits in Lechuguilla and Spider Caves. Environ Microbiol. 5:1071–1086.

Parchert K, Spilde MN, Porras-Alfaro A, Nyberg AM, Northrup DE. 2012. Fungal communities associated with rock varnish in Black Canyon, New Mexico: casual inhabitants or essential partners. Geomicrobiol. J. 29:752– 766.

Rawlings DE. 1999. Tributsch, H. Hansford, G.S. Reasons why '*Leptospirillum*'-like species rather than *Thiobacillus ferrooxidans* are the dominant iron-oxidizing bacteria in many commercial processes for the biooxidation of pyrite and related ores. Microbiol. 145:5-13.

Sayer JA, Cotter-Howells JD, Watson C, Hillier S, Gadd GM. 1999. Lead mineral transformation by fungi. Current Biol. 9:691-694.

Schrenk MO, Edwards KJ, Goodman RM, Hamers RJ, Banfield JF. 1998. Distribution of *Thiobacillus ferrooxidans* and *Leptospirillum ferrooxidans*: implications for generation of acid mine drainage. Science. 279:1519- 1522.

Schultze-Lam S, Fortin D, Davis BS, Beveridge TJ. 1996. Mineralization of bacterial surfaces. Chem Geol. 132:171-181.

Sharma PK, Capalash N, Kaur J. 2007. An improved method for single-step purification of metagenomic DNA. Mol Biotechnol. 36:61-63.

Spilde MN, Northup DE, Boston PJ, Schelble RT, Dano KE, Crossey LJ, Dahm CN. 2005. Geomicrobiology of cave ferromanganese deposits: a field and laboratory investigation. Geomicrobiol J. 22:99-116.

Urrutia MM, Beveridge TJ. 1994. Formation of fine-grained metal and silicate precipitates on a bacterial surface (*Bacillus subtilis*). Chem Geol. 116:261-280.

Wang X, Zeng L, Wiens M, Schloßmacher U, Jochum KP, Schröder HC, Müller WE. 2011. Evidence for a biogenic, microorganismal origin of rock varnish from the Gangdese Belt of Tibet. Micron. 42:401-411.

Figure legends

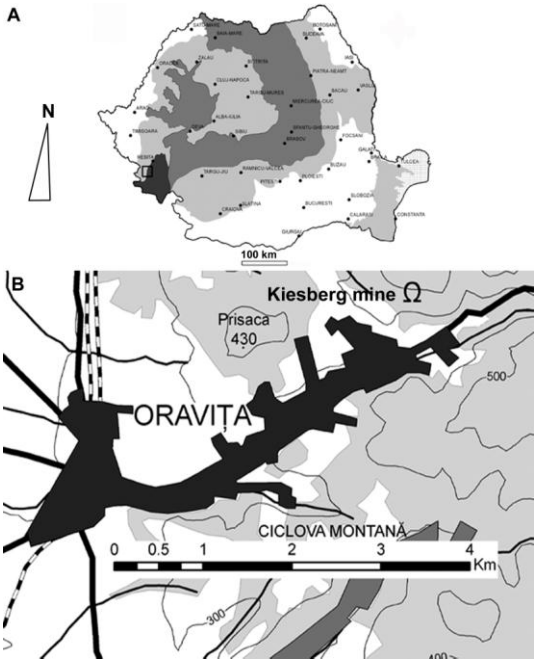

Fig. 1. Geographic location of the study area in **(A)** Romania and, more specifically, **(B)** the Oravita Region. The investigated Kiesberg Mine is indicated.

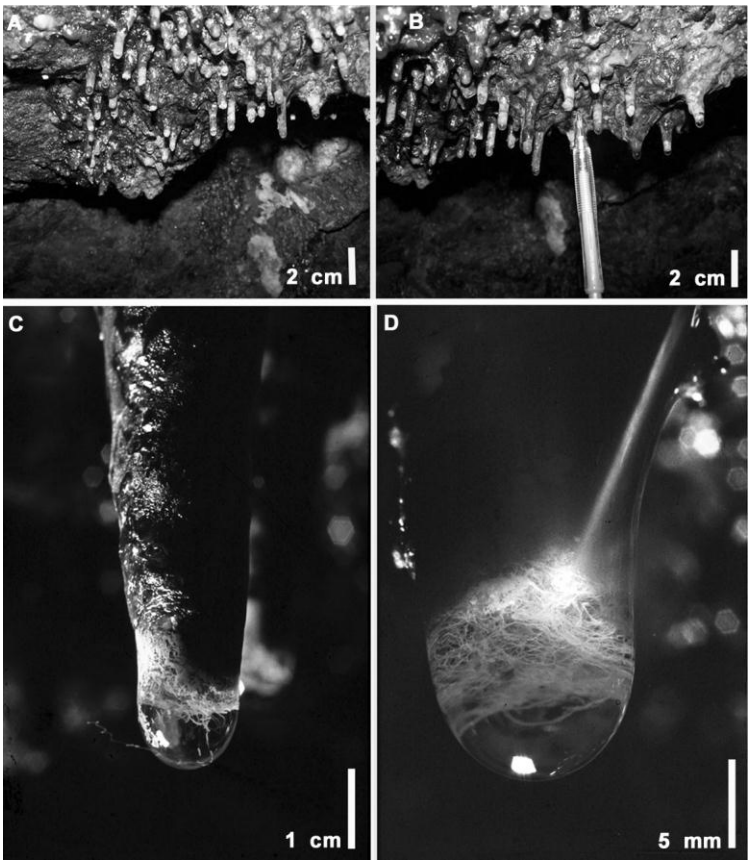

Fig. 2 (A) and **(B)** illustrate a typical formation of stalactites. **(C)** Close-up of a stalactite. **(D)** A drop of percolation solution at the tip of a stalactite with living fungi hyphae.

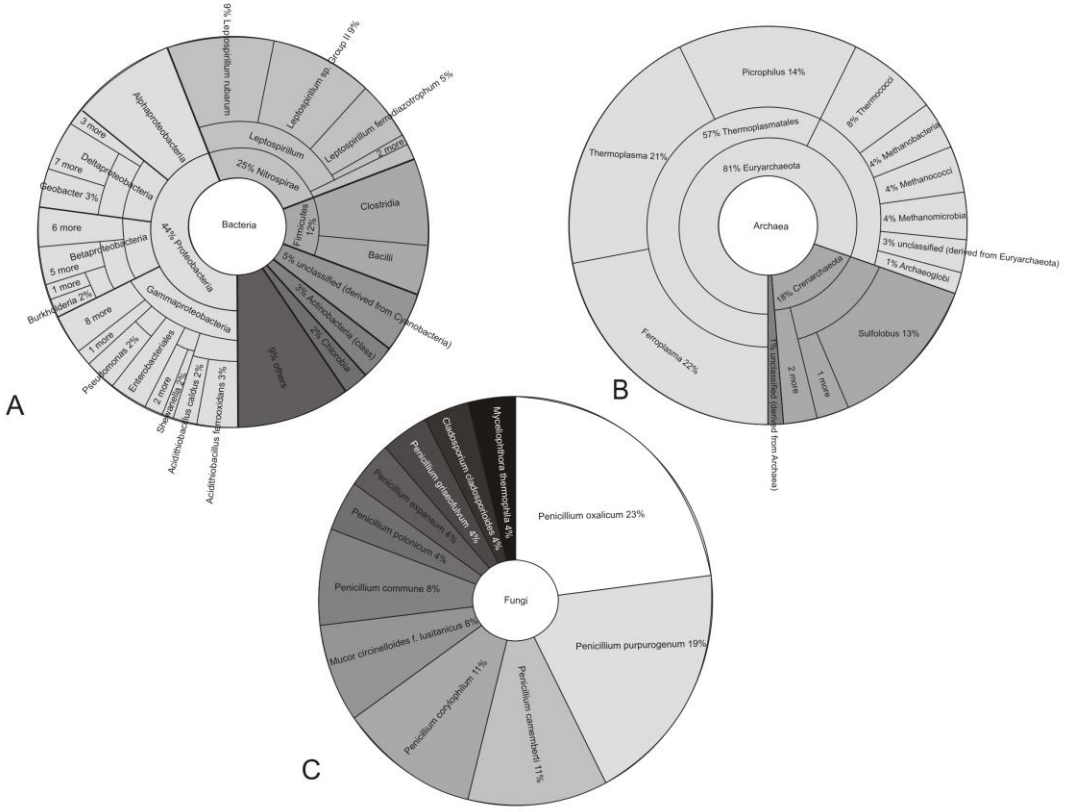

Fig. 3. Distribution of the bacterial **(A),** archaeal **(B)** and fungal **(C)** components of the percolation solution. Bacterial components are shown at various taxonomical levels, the identity of the major components (*Leptospirillum rubarum*, Leptospirillum sp. Group II, *Leptospirillum ferrodiazotrophum*, *Acidithiobacillus ferrooxidans* and *Acidithiobacillus caldus)* were confirmed at species level by manually reviewing sequence mapping to the reference 16S rRNA genes. Archaea are shown at genus level. Fungi are shown at species level confirmed by Sanger sequencing of 18S rRNA genes.

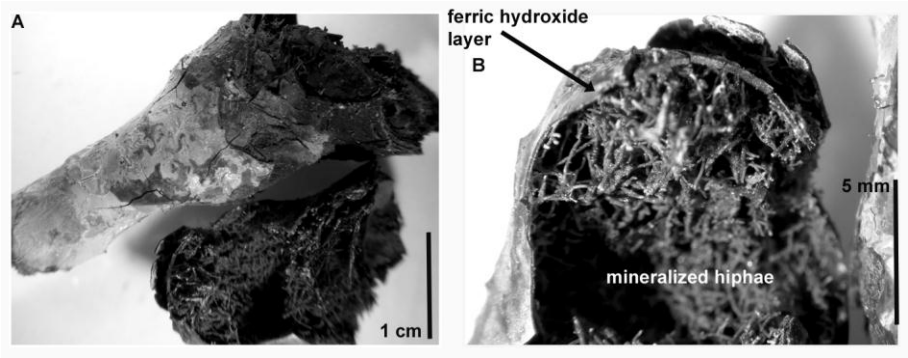

Fig. 4. Macroscopic analysis of a stalactite using a magnifying glass: **(A)** stalactite and **(B)** ferric hydroxide layer and mineralized hyphae.

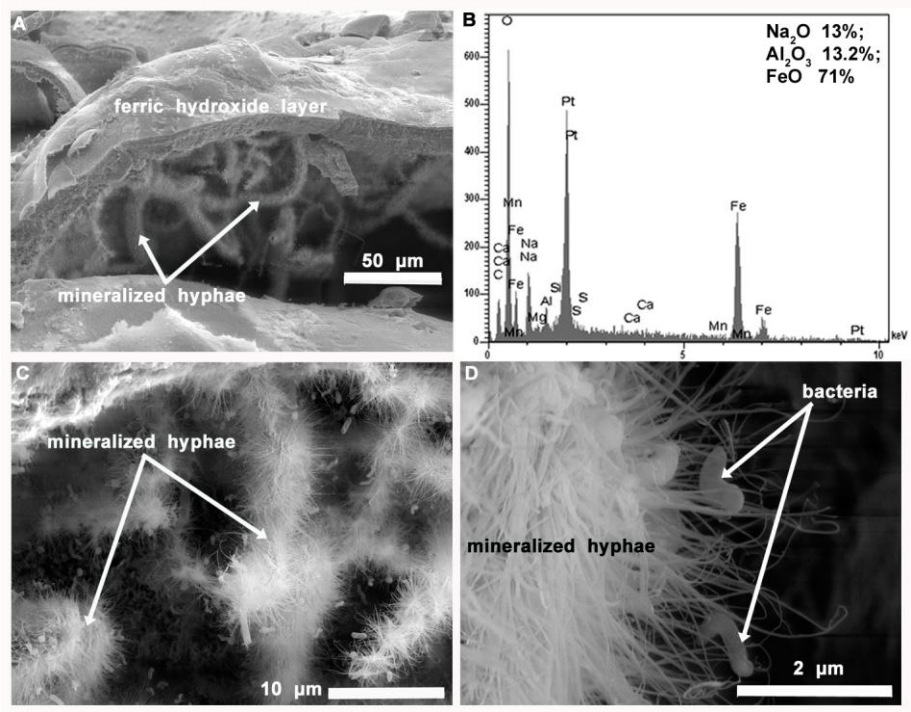

Fig. 5. (A) Microscopic view of ferric hydroxide layer and mineralized hyphae. **(B)** Atomic absorption spectrometry analysis of the ferric hydroxide layer. **(C)** and **(D)** Mineralized hyphae and bacteria.

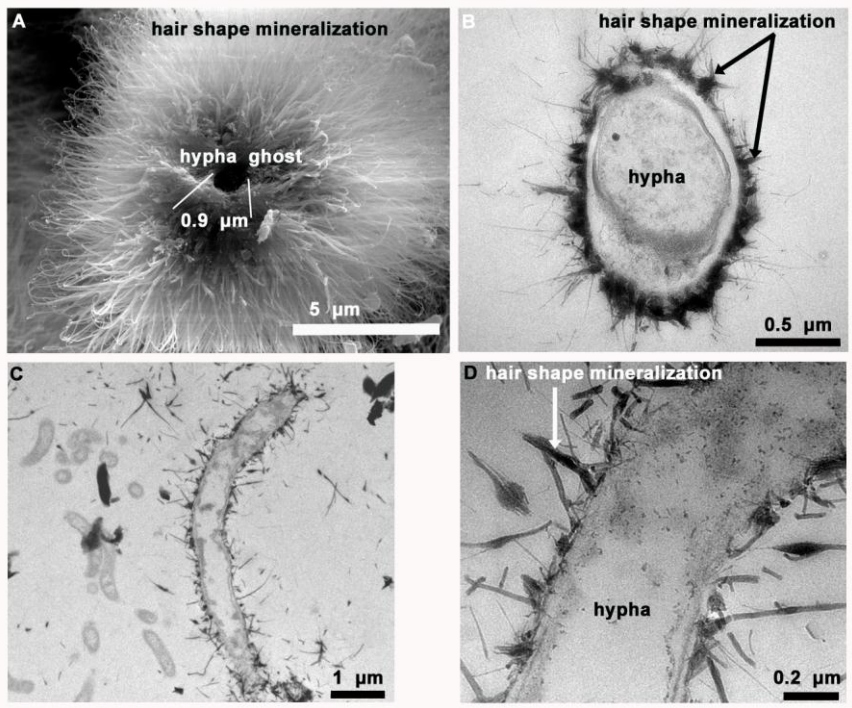

Fig. 6. (A) Hypha ghost (in SEM) surrounded by hair shape mineralization. **(B**–**D)** Living hyphae (sectioned at different levels in TEM) with hair-like mineralization of ferric hydroxide deposited on the cell wall.

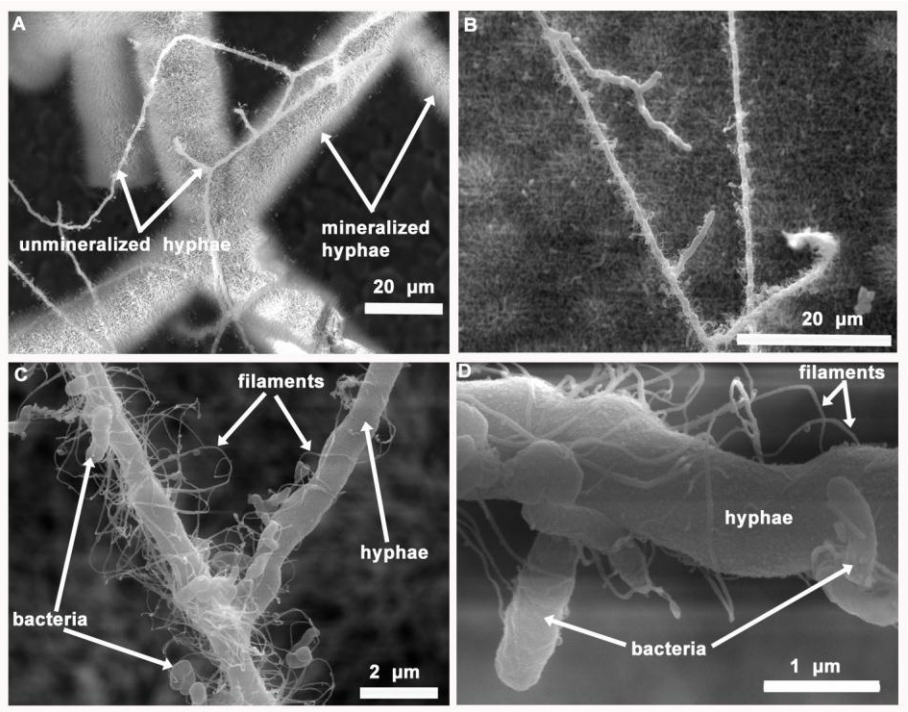

Fig. 7. (A) Microscopic view of mineralized hyphae and living unmineralized hyphae. **(B)** Microscopic view of living unmineralized hyphae. **(C)** and **(D)** Living unmineralized hyphae in direct contact with bacteria.

Table 1. Results of the atomic absorption spectroscopy analysis performed on the percolating solution (experimental errors were within 10 %).

	Fe	Na	K	Cr	Cd	Ni	Pb	Zn	Mn	Cu
mg L^{-1}	>15	30	22	0.227	0.08	1.18	0.04	2.9	>7.2	>10

Table 2. Abundance of bacterial and archaeal genera in the stalactite percolation solution based on metagenome mapping on 16S rDNA databases (SILVA SSU/ LSU, Greengenes and RDP). The relative abundance values (%) refer to the ratios of the genera in the total bacterial-archaeal ecosystem.

Bacteria						
Phylum	Class	Order	Family	Genus	Avg eValue	Abundance (%)
Nitrospirae	Nitrospira (class)	Nitrospirales	Nitrospiraceae	Leptospirillum	-13.24	24%
Proteobacteria	Gammaproteobacteria	Acidithiobacillales	Acidithiobacillaceae	Acidithiobacillus	-24.9	5%
Proteobacteria	Deltaproteobacteria	Desulfuromonadales	Geobacteraceae	Geobacter	-14.79	> 3%
Nitrospirae	Nitrospira (class)	Nitrospirales	Nitrospiraceae	Nitrospira	-12.58	< 2%
Proteobacteria	Betaproteobacteria	Burkholderiales	Burkholderiaceae	Burkholderia	-15.77	< 2%
Proteobacteria	Gammaproteobacteria	Pseudomonadales	Pseudomonadaceae	Pseudomonas	-14.93	< 2%
Chlorobi	Chlorobia	Chlorobiales	Chlorobiaceae	Chlorobium	-16.93	1-2%
Firmicutes	Bacilli	Bacillales	Bacillaceae	Bacillus	-8.48	> 1%
Proteobacteria	Gammaproteobacteria	Alteromonadales	Shewanellaceae	Shewanella	-13.18	> 1%
Cyanobacteria	unclassified (derived from Cyanobacteria)	Chroococcales	unclassified (derived from Chroococcales)	Synechococcus	-11.44	> 1%
Chlorobi	Chlorobia	Chlorobiales	Chlorobiaceae	Pelodictyon	-10.62	< 1%
Proteobacteria	Betaproteobacteria	Burkholderiales	Alcaligenaceae	Bordetella	-16.59	< 1%
Proteobacteria	Betaproteobacteria	Rhodocyclales	Rhodocyclaceae	Aromatoleum	-27.64	< 1%
unclassified (derived from Bacteria)	unclassified (derived from Bacteria)	unclassified (derived from Bacteria)	unclassified (derived from Bacteria)	unclassified (derived from Bacteria)	-11.92	< 1%
Acidobacteria	Solibacteres	Solibacterales	Solibacteraceae	Candidatus Solibacter	-10.46	< 1%
Cyanoba	unclassified	Nostocale	Nostocaceae	Nostoc	-23.72	< 1%

cteria	(derived from Cyanobacteria)	s				
Firmicutes	Clostridia	Clostridiales	Clostridiaceae	Clostridium	-12	< 1%
Firmicutes	Clostridia	Thermoanaerobacterales	Thermoanaerobacteraceae	Moorella	-16.78	< 1%
Proteobacteria	Alphaproteobacteria	Rhizobiales	Bradyrhizobiaceae	Bradyrhizobium	-11.23	< 1%
Proteobacteria	Betaproteobacteria	Burkholderiales	Comamonadaceae	Polaromonas	-16.04	< 1%
Proteobacteria	Deltaproteobacteria	Myxococcales	Myxococcaceae	Anaeromyxobacter	-17.42	< 1%
Proteobacteria	Deltaproteobacteria	Myxococcales	Myxococcaceae	Myxococcus	-9.29	< 1%
Proteobacteria	Deltaproteobacteria	unclassified (derived from Deltaproteobacteria)	unclassified (derived from Deltaproteobacteria)	unclassified (derived from Deltaproteobacteria)	-14.25	< 1%
Proteobacteria	Gammaproteobacteria	Alteromonadales	Alteromonadaceae	Marinobacter	-11.19	< 1%
Proteobacteria	Gammaproteobacteria	Chromatiales	Ectothiorhodospiraceae	Thioalkalivibrio	-6.65	< 1%
Aquificae	Aquificae (class)	Aquificales	Aquificaceae	Aquifex	-13.5	0-1%
Firmicutes	Bacilli	Bacillales	Bacillaceae	Geobacillus	-11.81	0-1%
Proteobacteria	Betaproteobacteria	unclassified (derived from Betaproteobacteria)	unclassified (derived from Betaproteobacteria)	Candidatus Accumulibacter	-10.7	0-1%
Proteobacteria	Deltaproteobacteria	Desulfobacterales	Desulfobacteraceae	Desulfobacterium	-5	0-1%
Proteobacteria	Deltaproteobacteria	Myxococcales	Cystobacteraceae	Stigmatella	-9.67	0-1%
Acidobacteria	unclassified (derived from Acidobacteria)	unclassified (derived from Acidobacteria)	unclassified (derived from Acidobacteria)	Candidatus Koribacter	-17.34	0-1%
Actinobacteria	Actinobacteria (class)	Actinomycetales	Nocardiaceae	Rhodococcus	-22	0-1%
Dictyoglomi	Dictyoglomia	Dictyoglomales	Dictyoglomaceae	Dictyoglomus	-12.75	0-1%
Firmicutes	Clostridia	Clostridiales	Heliobacteriaceae	Heliobacterium	-9.53	0-1%
Nitrospirae	Nitrospira (class)	Nitrospirales	Nitrospiraceae	Thermodesulfovibrio	-12.78	0-1%
Planctomycetes	Planctomycetia	Planctomycetales	Planctomycetaceae	Rhodopirellula	-6.93	0-1%

Poribacteria	unclassified (derived from Poribacteria)	unclassified (derived from Poribacteria)	unclassified (derived from Poribacteria)	unclassified (derived from Poribacteria)	-27.33	0-1%
Proteobacteria	Alphaproteobacteria	Rhizobiales	Bradyrhizobiaceae	Nitrobacter	-11.8	0-1%
Proteobacteria	Alphaproteobacteria	Rhizobiales	Bradyrhizobiaceae	Rhodopseudomonas	-25.71	0-1%
Proteobacteria	Betaproteobacteria	Burkholderiales	Burkholderiaceae	Cupriavidus	-11.67	0-1%
Proteobacteria	Betaproteobacteria	Burkholderiales	Burkholderiaceae	Ralstonia	-8	0-1%
Proteobacteria	Betaproteobacteria	Rhodocyclales	Rhodocyclaceae	Dechloromonas	-6.29	0-1%
Proteobacteria	Deltaproteobacteria	Desulfobacterales	Desulfobacteraceae	Desulfococcus	-5.25	0-1%
Proteobacteria	Deltaproteobacteria	Desulfuromonadales	Pelobacteraceae	Pelobacter	-18.22	0-1%
Proteobacteria	Deltaproteobacteria	Syntrophobacterales	Syntrophobacteraceae	Syntrophobacter	-14.49	0-1%
Proteobacteria	Epsilonproteobacteria	Campylobacterales	Helicobacteraceae	Helicobacter	-27.6	0-1%
Archaea						
Phylum	Class	Order	Family	Genus	Avg eValue	Abundance (%)
Euryarchaeota	Thermoplasmata	Thermoplasmatales	Thermoplasmataceae	Thermoplasma	-11.92	< 3%
Euryarchaeota	Thermoplasmata	Thermoplasmatales	Ferroplasmaceae	Ferroplasma	-16.81	> 2%
Euryarchaeota	Thermoplasmata	Thermoplasmatales	Picrophilaceae	Picrophilus	-9.5	2%
Crenarchaeota	Thermoprotei	Sulfolobales	Sulfolobaceae	Sulfolobus	-9.88	< 2%
Euryarchaeota	Methanococci	Methanococcales	Methanocaldococcaceae	Methanocaldococcus	-5.84	0-1%